Analytical Methods

Accepted Manuscript

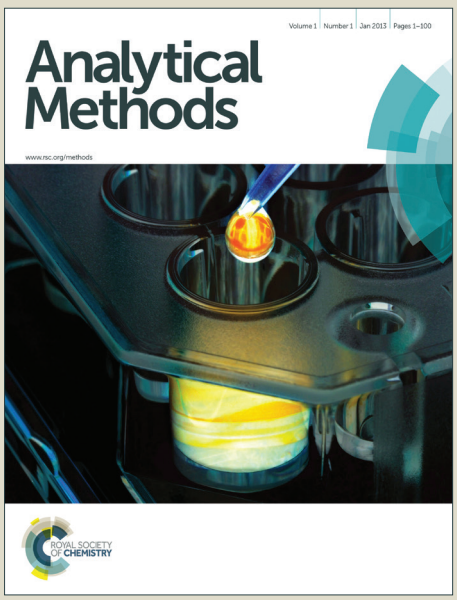

ROYAL SOCIETY OF CHEMISTRY

www.rsc.org/methods

Simultaneous voltammetric determination of ascorbic acid and uric acid using seven-hole carbon nanotubes paste multielectrode array

Yage Peng,[*a,b,] Dongdong Zhang,[c] Chengxiao Zhang [b]

[a] *School of Chemistry and Chemical Engineering, Ningxia University, Ningxia, Yinchuan, 750021(P. R.China)*

[b] *Key Laboratory of Applied Surface and Colloid Chemistry, Ministry of Education, School of Chemistry and Chemical Engineering, Shaanxi Normal University, Xi'an 710062 (PR China)*

[c] *School of Medicine, Xi'an Jiaotong University, Xi'an 710061, P.R. China*

∗To whom correspondence should be addressed. E-mail: yagepeng@126.com

Phone: +86-951-2062004; Fax: 86-951- 2062860.

ABSTRACT

In this study, a seven-hole multielectrode array comprising of six carbon nanotubes paste working electrodes and a carbon nanotubes paste counter electrode (Fig. 1) was designed and fabricated. To reduce sample consumption, a novel 'micro-drop' cell including an Ag/AgCl micro-reference electrode was fabricated for simultaneous determination of ascorbic acid and uric acid via cyclic voltammetry (CV) and square wave voltammetry (SWV) at the multielectrode array fabricated. In the simultaneous detection of the ascorbic acid and uric acid using CV at carbon nanotubes paste working electrodes, the oxidation peak separation of ascorbic acid and uric acid increased from 0.09 V to 0.15 V and the oxidation peak currents of ascorbic acid and uric acid greatly enhanced compared with carbon paste working electrodes, respectively. Under the optimized conditions, the oxidation peak currents were linear over ranges from 2.0×10^{-6} M to 8.0×10^{-4} M for ascorbic acid in the presence of 6.0×10^{-6} M uric acid, and from 2.0×10^{-7} M to 8.0×10^{-5} M for uric acid in the presence of 2.0×10^{-4} M ascorbic acid, with the detection limits of 1.0×10^{-6} M and 9.0×10^{-8} M(S/N = 3), respectively. The effect of potential interferences including compounds usually found in human fluids (L-lysine, glucose, citric acid, glycin and cystine) were examined. The proposed method has been successfully applied to the determination of ascorbic acid and uric acid in human urine with satisfactory result. This work demonstrates that the carbon nanotubes paste multielectrode array is a promising strategy for simultaneous electrochemical determination of isomers of organic compounds.

Keywords: Multielectrode array; Paste electrode; Carbon nanotubes; Ascorbic acid; Uric acid

1. Introduction

Multielectrode arrays have been received a great deal of attention due to its versatility and potential advantages over more single electrode, such as less sample, high throughput, low cost per test, and much more analytical information to elucidate multiple events.[1] Mutielectrode arrays have been widely applied in environmental analysis,[2] food analysis,[3,4] clinical diagnostics,[5,6] immunoassay,[7,8] DNA assay[9,10] and aptasensor.[11]

Much effort has been devoted to design novel multielectrode arrays in order to expand the applications of multielectrode arrays in many fields. These include design of different electrode configures such as strip,[9] interdigitated[5], discal[11] and quadrate,[12] increase of the amount of electrodes, miniaturization of the size of electrodes and decrease of the cost of the electrodes. In addition, employment of different substrate materials such as silicon,[13] glass,[10] ceramic and polymer,[9] and utilization of different electrode materials such as carbon,[10] gold,[5,12] platinum and iridium oxide[11] were applied. However, the above-mentioned electrode arrays were mainly obtained through complex and expensive industrial or laboratory procedures, such as photolithography or metal deposition. So, particular attention has been given to a simple and inexpensive methods used to obtain the surface-renewable electrode array.

In recent years, application of nanomaterials in multielectrode arrays reveals a great sensitivity and selectivity in the developed analytical methods.[14,15] Carbon nanotubes (CNT), initially discovered by Iijima,[16] consisting of cylindrical graphene sheets with nanometer diameter, have attracted much attention due to their unique mechanical, chemical, electrochemical properties such as broad potential window and low background current. Multi-wall carbon nanotubes (MWNT) coated electrodes and MWNT paste electrodes exhibited the excellent electrochemically catalytic properties

to biological active substances, such as ascorbic acid, uric acid, dopamine,[17] norepinephrine and epinephrine.[18]

Ascorbic acid (AA) is a vital vitamin in the diet of humans and is present in mammalian brain along with several neurotransmitter amines. Ascorbic acid has been used for the prevention and treatment of common cold, mental illness, infertility, cancer and acquired immune deficiency syndrome.[19] Uric acid (UA) is the primary end product of purine metabolism. It has been shown that the extreme abnormalities of UA levels in the body are symptoms of several diseases, such as gout, hyperuricemia, and Lesch–Nyhan syndrome.[20] As AA and UA are coexistent in biological fluids of urine and serum, it holds great importance to develop a simple technique to simultaneously detect UA and AA.[21] However, the electrochemical determination of AA and UA in samples gives rise to mutual interferences because the oxidation potentials of them at conventional electrodes are so near that they are difficult to separate their voltammetric peaks. Therefore, it is essential to develop simple and rapid methods for their determination in routine analysis without cross interferences.

Considerable efforts have been devoted to develop simple and rapid electrochemical methods for simultaneous determination of AA and UA. They are involving single modified electrode including chemical/polymer modified electrodes such as 2,5-dimercapto-1,3,4-thiadiazole,[22] caffeic acid,[23] polycalconcarboxylic acid,[24] poly(acid chrome blue K)[25] and poly(p-xylenolsulfonephthalein);[26] nano-material modified electrodes such as helical carbon nanotubes[27] and iron(III)-porphyrin functionalized multi-walled carbon nanotubes;[28] metal oxide modified electrodes such as hydrous ruthenium oxide film[29] and copper modified electrode;[30] graphene modified electrode such as screen-printed graphene electrode[31]

and reduced graphene oxide films modified electrode.[32] However, to our best knowledge, carbon nanotubes paste multielectrode array to simultaneous voltammetric determination of ascorbic acid and uric acid have not been reported.

The aim of the present work is to design a novel carbon nanotubes paste multielectrode array for the application in simultaneous determination of AA and UA, which were chosen as model multiple analytes. In this paper, a multielectrode array was designed and the electrochemical characteristics of carbon nanotubes paste electrode were investigated. A simple electrochemical method for simultaneous determination of AA and UA at the carbon nanotubes paste electrode was presented.

2. Experimental

2.1. Materials and reagents

Uric acid (UA) was purchased from Sigma-Aldrich (USA). L-ascorbic acid (AA), L-lysine, glucose, citric acid, glycin, cystine, graphite powder (particle size＜100 μm) and mineral oil were obtained from Xi'an Chemical Reagent Company (Xi' an, China). Silver powder was obtained from Hubei Huitian Adhesive Enterprise Co., Ltd (Hubei, China). Multi-wall carbon nanotubes (MWNT) were obtained from Shenzhen Nanotech Port Co. Ltd. (Shenzhen, China). The MWNT purchased was ultrasonically treated in a mixed solution of nitric acid and perchloric acid (V/V 7:3) to remove graphitic nanoparticles, amorphous carbon and catalyst impurities present and to be functionalized with carboxylic acid groups according to micro-reference.[33] All reagents were of analytical grade and used without any further purification. Ultrapure water (18.2 MΩ.cm) from a Millipore system was used for preparing all the solutions.

Seven-hole 1, 2, 3, 4, 5, 6 (inner diameter = 0.80 mm) and 7 (inner diameter = 1.6 mm)) polymethylmethacrylate cylinder (diameter = 0.60 cm, length = 2.5 cm) was friendly provided by Xi'an Institute of Optics and Precision Mechanics of Chinese

Academy of Sciences (Xi'an, China).

The stock solution of AA (0.010 M) was prepared daily by dissolving AA solid in ultrapure water and diluted to desired concentration with 0.10 M acetate buffer solution (pH 5.00). The stock solution of UA (0.0010 M) was prepared by dissolving UA solid in 0.1 M sodium hydroxide and diluted to desired concentration with 0.10 M acetate buffer solution (pH 5.00).

2.2. Apparatus

Electrochemical measurements were performed on a CHI 1030 multichannel electrochemical workstation (CH Instruments, Shanghai Chenhua Instrument Corporation, China). A three-electrode system was employed, composing of carbon nanotubes paste multielectrode array or graphite paste multielectrode array as working electrode, an Ag/AgCl micro-reference electrode (sat. KCl) as the micro-reference electrode, and a carbon nanotubes paste electrode as the counter electrode. All potentials were referred to this micro-reference electrode.

2.3. Preparation of multielectrode array

Fig. 1 shows the schematic diagram of the multielectrode array used in this work, consisting of six carbon nanotubes paste working electrodes and a carbon nanotubes paste counter electrode. The multielectrode array was prepared by hand-mixing the pretreated MWNT powder with mineral oil in a ratio of 3:2 in an agate mortar,[33] and then a portion of the mixed paste was packed firmly into the each cavity of a seven-hole polymethylmethacrylate cylinder. Finally, the electric contact was established by inserting a copper wire (diameter = 0.10 mm, length = 90 mm) down into the each hole.[33]

For comparison, the graphite paste multielectrode array was prepared with the same procedure as that for the carbon nanotubes paste multielectrode array by mixing

80% graphite powder with 20% mineral oil (w/w).

A new surface of the multielectrode was obtained by smoothing the electrode on weighing paper. The as-prepared electrodes was pretreated by applying a scan potential from 0 to +1.5 V at a scan rate of 100 mV s^{-1} in 0.10 M phosphate buffer saline (pH 7.40) for 10 min until a stable response was obtained.[33]

2.4. Electrochemical measurement

The schematic diagram of electrochemical measurement system the including six carbon nanotubes paste working electrodes, a carbon nanotubes paste counter electrode, an Ag/AgCl micro-reference electrode and the 'micro-drop' cell is shown in Fig.1.

The 'micro-drop' cell showed Fig. 1 was constructed by following three steps. Firstly, the multielectrode array fabricated with above-described protocol was held upside down. Secondly, 50 μL of 0.10 M acetate buffer solution (pH 5.00) containing the single or mixed components of AA and UA was dropped onto the surface of the multielectrode array to merging all electrodes surface. Finally, an Ag/AgCl micro-reference electrode (sat. KCl) was gingerly inserted into the 50 μL acetate buffer solution. After the each electrochemical measurement was performed, the 'micro-drop' cell was taken away by rubber pipette bulb, and then a new 'micro-drop' cell was restructured by dropping 50 μL of buffer solution.

Cyclic voltammetry (CV) was performed with a scan rate of 50 mV s^{-1} in the potential range from -0.10 to 0.80 V. Square wave voltammetry (SWV) was carried out in the potential range from -0.10 to 0.80 V with amplitude of 25 mV, step potential, 4.0 mV, at 15 Hz impulse frequency unless otherwise stated. All electrochemical experiments were carried out at room temperature (25±1℃).

The application of the multielectrode array to determine the UA content in

human urine samples and the AA content in human serum sample was studied.

3. Results and discussion

3.1. Design of the electrochemical cell

Design of the electrochemical cell is one of the most important aspects for the biosensor array. In the design of the electrochemical cell for the biosensor array, the following factors should be kept in mind. First, the cell must be designed to be easy in exchanging electrodes or biosensors. Secondly, the cell should be suitable for trace analysis. Finally, it should have the great analytical characteristics, such as a fast response, a wide linear range and a low detection limit. But, the conventional cell is usually a covered beaker of 5-50 mL volume and contains the three electrodes (working, reference, and auxiliary), which are immersed in the sample solution. So it needs at least 2.0 mL the sample solution and is unsuitable for trace analysis. On the other hand, the conventional cell is inconvenient in exchanging electrodes or biosensors. Thus, the conventional cell was replaced by the novel 'micro-drop' cell for the multielectrode array in this paper.

A novel 'micro-drop' cell was designed according to the above-mentioned three factors. This design favors an exchanging biosensor, avoiding contamination of the sensing surface, and reducing the sample volume. The electrochemical behavior difference of the 50 μL 'micro-drop' cell designed and the conventional 2.0 mL cell was examined by cyclic voltammetry in 0.10 M PBS（pH 7.40）solution contained 1.0×10^{-3} M $K_3[Fe(CN)_6]$ and 0.10 M KCl. The cyclic voltammograms of $K_3[Fe(CN)_6]$ showed that the peak potentials in the 'micro-drop' cell were as same as those in the conventional cell. But, the peak currents were higher than that in the conventional cell. This is attributed to the fact that the working electrode and micro-reference electrode at the 'micro-drop' cell has closer distance than that the conventional cell, so, the

resistance of them is smaller than that the conventional cell. A satisfactory design of the electrochemical cell is, therefore, evident.

3.2. Electrochemical behaviors of the multielectrode array fabricated

The graphite paste multielectrode array and the carbon nanotubes paste multielectrode array fabricated were electrochemical characterized by cyclic voltommtery in 0.10 M PBS（pH 7.40）solution contained 1.0×10^{-3} M $K_3[Fe(CN)_6]$ and 0.10 M KCl from -0.1 to 0.6 V at a scan rate of 50 $mV.s^{-1}$. The cyclic voltammograms obtained at three graphite paste working electrodes (dot line) and three carbon nanotubes paste working electrodes (solid line) are showed in Fig. 2. From Fig. 2, the average of the peak potential separation ($\triangle E_p$) at the graphite paste multielectrode array and the carbon nanotubes paste multielectrode array is ~107 mV and ~79 mV, and the average ratio of oxidation peak currents to reduction peak currents (I_{pa}/I_{pc}) is ~1.0. This indicates that a close reversible electron transfer process can be obtained at the both graphite paste and carbon nanotubes multielectrode array.[34] Furthermore, the peak currents at carbon nanotubes paste multielectrode array were 1.8 folds higher than that at graphite paste multielectrode array. In order to explain this result, two experiments, the active surface areas and the capability of electron transfer in graphite paste electrode and carbon nanotubes paste electrode, were performed. First, the active surface areas of graphite paste electrode and carbon nanotubes paste electrode were calculated from a slope of the i vs. $v^{1/2}$ plot using the *Randles-Sevcik* equation, in 0.10 M KCl-1.0×10^{-3} M $K_3[Fe(CN)_6]$ ($D = 7.6 \times 10^{-6}$ $cm^2.s^{-1}$).[35] The active surface area of graphite paste was 0.0061 cm^2. The carbon nanotubes paste active surface area of was 0.0080 cm^2, which is 1.3-fold that of graphite paste. This indicates that carbon nanotubes can increase the active surface area. Second, the capability of electron transfer in graphite paste electrode and carbon

nanotubes paste electrode was checked by AC impedance spectroscopy in 0.10 M PBS (pH 7.40) containing 2.0×10^{-3} M $K_3Fe(CN)_6$-2.0×10^{-3} M $K_4Fe(CN)_6$. The result showed that the charge transfer resistance for carbon nanotubes paste electrodes was notably reduced compared with graphite paste. This indicates that the carbon nanotubes improves the electronic and ionic transport capability, attributed to that the carbon nanotubes provide a three-dimensional electron-conductive network, which extended throughout the ion-conductive matrix of multielectrode array.[36] It is most important that the relative standard deviations of the peak currents obtained at three channels of graphite paste multielectrode array and three channels of carbon nanotubes paste multielectrode array are less than 1.5%. This indicates that both graphite paste multielectrode array and the carbon nanotubes paste multielectrode array showed excellent stability and can be utilized as working multielectrodes for following experiments.

3.3. Electrochemical behaviors of AA and UA at multielectrode array

3.3.1. Single composition of AA and UA at multielectrode array

Fig. 3 shows the cyclic voltammograms of AA (Fig. 3 A) and UA (Fig. 3 B) at a scan rate of 50 $mV.s^{-1}$ in 0.10 M acetate buffer solution (pH 5.00) at three graphite paste working electrodes (dot line) and three carbon nanotubes paste working electrodes (solid line), respectively.

From Fig. 3 A, the anodic peak potential of AA appears at 0.47 V on the graphite paste electrode and at 0.34 V on the carbon nanotubes paste electrode, respectively. The anodic potential of AA negatively shifted 0.13 V on the carbon nanotubes paste electrode, compared with that on the graphite paste electrode. This indicates that the electrocatalytic oxidation of AA occurred in the presence of MWNT, which is consistent with the report by Rivas.[17] The anodic peak current of AA at carbon

nanotubes paste is 6 folds higher than that at the graphite paste electrode.

From Fig. 3 B, it can be seen that the anodic peak potential of UA oxidation at carbon nanotubes paste electrode appears at about 0.48 V as the same as at graphite paste electrode. No cathodic peak is observed on the reverse potential scan at graphite paste electrode or carbon nanotubes paste electrode, suggesting that the electrode reaction of UA is irreversible. From Fig. 3 B, it is obviously seen about 5-fold enhanced anodic peak current of UA at carbon nanotubes paste electrode.

The increase of the anodic peak currents of AA and UA at carbon nanotubes paste electrode is attributed to the fact that the active surface area and the capability of electron transfer of the carbon nanotubes paste electrode significantly increase compared with that of the graphite paste electrode.

3.2.2. The mixtures of AA and UA at multielectrode array

Fig. 4 shows the cyclic voltammograms of a mixture of AA and UA at three graphite paste electrodes (dot line) and at three carbon nanotubes paste electrodes (solid line) at a scan rate of 50 mV s^{-1} in 0.10 M acetate buffer solution (pH 5.00), respectively. From Fig. 4 (dot line), it can be seen that the oxidation peaks of AA and UA appeared at 0.39 V and 0.48 V at graphite paste electrode, respectively. In contrast, AA and UA yielded two well-defined oxidation peaks at carbon nanotubes paste electrode (solid line), whose peak potentials were 0.33 V and 0.48 V, respectively. Meanwhile, the oxidation peak currents also remarkably increased at carbon nanotubes paste electrode. It is no doubt that the increase in currents and separation peak potential arise from MWNT (functionalized with carboxylic acid groups) due to its high surface area possessing abundant acidic sites, which can offer special approach to the simultaneously electrochemical determination of AA and UA.

3.2.3. Effect of pH on the oxidation of AA and UA in a mixture

Effect of pH on the peak currents of the AA (pK_a=4.17) and UA (pK_a=5.75) in a mixture was checked using cyclic voltammetry between -0.10 V and 0.80V at carbon nanotubes paste electrode in 0.10 M acetate buffer (pH 3.80-5.80). Fig. 5 illustrates the dependence of the oxidation peak currents of AA and UA on pH of the supporting electrolyte solution. From Fig. 5, it can be seen that the oxidation peak current of AA increases slightly with an increase of pH from 3.80 to 4.20 and no obvious changes in the peak currents of AA are observed over the pH range from 4.20 to 5.00. For UA, the anodic peak currents increases with increasing pH until pH reaches 5.00. At a pH higher than 5.00, the oxidation peak currents of AA and UA decrease with increasing pH. The effect of pH on peak currents of AA and UA may result from electrochemical oxidation processes of AA and UA and their adsorption at the carbon nanotubes paste electrode. At low pH, efficient electrochemical oxidation processes of AA and UA increase with an increase of pH. Both AA and UA exist mostly in anionic form at pH higher than 5.40 and 4.10, which are the pK_a values of UA and AA, respectively, at 25±1℃. On the other side, UA is known to be protic aromatic molecules and can become deprotonated as anions at higher pH. Therefore, with the increase in pH, the oxygen-containing functional groups at the carbon nanotubes paste electrode may become deprotonated and possessed negative charges. Electrostatic repulsion between the analytes and the electrode might be one of the reasons that the adsorptions of analytes on the electrode at higher pH are inefficient.

Effect of pH on the peak potentials of the AA and UA in a mixture at carbon nanotubes paste electrode was also studied. The results showed that both the anodic peak potentials of AA and UA shifted negatively with the increase of pH from 3.80 to 5.80. The equations of peak potential with the pH were obtained, for AA: E_{pa} = -49.2pH + 448.7 (mV, r =0.9983); for UA: E_{pa} = -57.9 pH + 765.4 (mV, r = 0.9980).

Considering the favorable peak current and the large peak separation between these two compounds, a befitting pH 5.00 was selected for the simultaneous detection of AA and UA.

3.4. Simultaneous Determination of AA and UA

In order to improve sensitivity, linear sweep voltammetry and square wave voltammetry (SWV) were employed, respectively. It was found that a large separation peak potential and a high sensitivity were obtained by employing SWV. Therefore, SWV was used in this work because of its excellent sensitivity. The electrochemical parameters for SWV simultaneous determination of AA and UA on the carbon nanotubes paste electrode were optimized. Considering the sensitivity and selectivity, 15 Hz impulse frequency, 25 mV amplitude and 4.0 mV step potential were chosen in the following experiment.

Fig. 6 A shows the SW voltammograms of AA from 2.0×10^{-6} to 8.0×10^{-4} M in the presence of 6.0×10^{-6} M UA. From an inset calibration plot of AA in Fig. 6 A, it is also seen that the peak current of AA was linear with the concentration of AA in the range from 2.0×10^{-6} to 8.0×10^{-4} M in the presence of 6.0×10^{-6} M UA. The regression equation was I (μA) = (0.0530±0.0104) + (0.0170±0.0003) C (10^{-5} M), r = 0.9982, and the detection limit (S/N = 3) was 1.0×10^{-6} M. The relative standard deviation of one channel in five successive scans is 3.1% at 2.0×10^{-5} AA, and the relative standard deviation of six channels is 1.4% for 2.0×10^{-5} AA.

Fig. 6 B shows the SW voltammograms of UA from 2.0×10^{-7} to 8.0×10^{-5} M in the presence of 2.0×10^{-4} M AA. Under the optimized condition, the peak current of UA was linear with the concentration of UA in the range from 2.0×10^{-7} to 8.0×10^{-5}M in the presence of 2.0×10^{-4} M AA (Fig. 6 B, inset). The regression equation was I (μA) = (0.4602±0.0236) + (0.0442±0.0008) C (10^{-5} M), r = 0.9983, the detection limit for

UA was 9.0×10^{-8} M (*S/N* = 3). The relative standard derivation was 1.74% for five successive assays at 2.0×10^{-6} M UA, and the relative standard deviation of six channels is 1.0% for 2.0×10^{-6} UA.

3.5. Surface-renewal of the electrode

The main attraction of using the paste electrode is that the electrode surface can be renewed very easy after every use. The carbon nanotube paste multielectrode array (carbon nanotubes paste electrode) can be renewed by squeezing a little carbon nanotube paste out of the cylinder and a fresh surface is smoothed on a piece of weighing paper whenever needed.[37]

To test paste homogeneity, the carbon nanotubes paste electrode fabricated was applied for 2.0×10^{-5} M UA measurement in 0.10 M acetate buffer solution (pH 5.00). The measurement was repeated five times and after each measurement the electrode surface was renewed as explained above. The relative standard deviation of the peak current of one channel was 4.1%.

3.6. Interference study

The influence of various possible interferents was tested under the optimized conditions by analyzing a standard solution of 2.0×10^{-4} M AA and 2.0×10^{-5} M UA. The tolerable limit of a foreign species was taken as a relative error less than 5%. The tolerated concentration of foreign substances was 0.050 M for Mg^{2+} and Ca^{2+}, 5.0×10^{-3} M for L-lysine, glucose, citric acid, glycin and cystine. A satisfactory selectivity of the proposed method was therefore evident.

3.7. Analysis of real samples

To verify the practicality of the carbon nanotube paste mutilelectrode array fabricated, the proposed method has been applied to the direct determination of uric acid in buffer solutions of human urine and serum samples. The human urine and

serum samples were diluted 100 and 10 times with acetate buffer solutions (0.10 M, pH 5.00) before the measurements, respectively. The standard addition method was used for the analysis of the prepared samples. The recovery ratio based on this method was listed in Tables 1. When known amounts of UA were added to the urine samples, quantitative recoveries of 100%-104% were obtained. When known amounts of UA were added to the serum samples, quantitative recoveries of 97%-99% were obtained. Comparisons of the proposed method with reference methods,[38-41] also confirmed the accuracy of the results obtained by our proposed method, showing no significant differences from those of the reported method.

4. Conclusion

Carbon nanotube paste multielectrode array with six small working electrodes, a big counter electrode and a reference has been designed and fabricated. A simple and rapid electrochemical method for simultaneous determination of ascorbic acid and uric acid at the multielectrode array and 'micro-drop' cell designed has been developed. This work demonstrates that the carbon nanotube paste multielectrode array fabricated incorporating 'micro-drop' cell and multi-channel electrochemical technique is a promising strategy for multicomponent analysis. Compared with other electrode array patterns or designs, the fabricated procedure and the surface-renewable method of the carbon nanotube paste multielectrode array in this work are very simple, and the manufacture costs of multielectrode array is greatly reduced. Moreover, the multielectrode array and 'micro-drop' cell designed requires fewer samples, increase the test throughput and reduce the cost per test. The multielectrode array concept and 'micro-drop' cell described in this paper may have value in the simultaneous analysis of multiple analytes.

ACKNOWLEDGEMENTS

The authors gratefully acknowledge the financial support of the National Natural Science Foundation of China (21005003, 21305106).

References

1 A. P. Deng and H. Yang, *Sens. Actuators, B,* 2007, **124**, 202–208.

2 S. Carroll and R. P. Baldwin, *Anal. Chem.*, 2010, **82**, 878–885.

3 S. Piermarini, L. Micheli, N. H. S. Ammida, G. Palleschi and D. Mosconea, *Biosens. Bioelectron*., 2007, **22**, 1434–1440.

4 C. O. Parker, Y. H. Lanyon, M. Manning, D. W. M. Arrigan and I. E. Tothill, *Anal. Chem.*, 2009, **81**, 5291–5298.

5 J. Yan, V. A. Pedrosa, A. L. Simonian and A. Revzin, *Appl. Mater. Interfaces*, 2010, **2**, 748–755.

6 F. Y. Kong, B. Y. Xu, Y. Du, J. J. Xu and H. Y. Chen, *Chem. Commun.*, 2013, **49**, 1052–1054.

7 D. P. Tang, J. Tang, B. L. Su, J. J Ren and G. N. Chen, *Biosens. Bioelectron*., 2010, **25**, 1658–1662.

8 W. C. Dou, W. L. Tang and G. Y. Zhao, *Electrochem. Acta*, 2013, **97**, 79–85.

9 D. D. Zhang, Y. G. Peng, H. L. Qi, Q. Gao and C. X. Zhang, *Biosens. Bioelectron*., 2010, **25**, 1088–1094.

10 X. Zhu, K. Ino, Z. Y. Lin, H. Shiku, G. N. Chen and T. Matsue, *Sens. Actuators, B*, 2011, **160**, 923–928.

11 Y. Du, C. G. Chen, J. Y. Yin, B. L. Li, M. Zhou, S. J. Dong and E. K. Wang, *Anal. Chem.*, 2010, **82**, 1556–1563.

12 L. Civit, A. Fragosoa, S. Höltersb, M. Dürstb and C. K. O'Sullivana, *Anal. Chim. Acta*, 2012, **715**, 93–98

13 X. J. Chen, S. Roy, Y. F. Peng and Z. Q. Gao, *Anal. Chem.*, 2010, **82**, 5958–5964.

14 D. D. Zhang, Y. G. Peng, H. L. Qi, Q. Gao and C. X. Zhang, *Sens. Actuators, B*, 2009, **136**, 113–121.

15 G. M. Yang, Y. Q. Chen, L. Li and Y. H. Yang, *Clin. Chim. Acta*, 2011, **412**, 1544–1549.

16 S. Iijima, *Nature*, 1991, **354**, 56–58.

17 M. D. Rubianes and G. A. Rivas, *Electrochem. Commun.*, 2003, **5**, 689–694.

18 M. Chicharro, A. Sánchez, E. Bermejo, A. Zapardiel, M. D. Rubianes and G. A. Rivas, *Anal. Chim. Acta*, 2005, **543**, 84–91.

19 O. Arrigoni and C. D. Tullio, *Biochim. Biophys. Acta, Rev.*, 2002, **1569**, 1–9.

20 B. Ullman, M. A. Wormsted, M. B. Cohen and D. W. Martin Jr, *Proc. Natl. Acad. Sci.*, 1982, **79**, 5127–5131.

21 J. M Zen and J. S. Tang, *Anal. Chem.*, 1995, **67**, 1892–1895.

22 P. Kalimuthu and S. Abraham John, *Electrochem. Commun.*, 2005, **7**, 1271–1276.

23 W. Ren, H. Q. Luo and N. B. Li, *Biosens. Bioelectron*., 2006, **21**, 1086–1092.

24 A. L. Liu, S. B. Zhang, W. Chen, X. H. Lin and X. H. Xia, *Biosens. Bioelectron*., 2008, **23**, 1488–1495.

25 R. Zhang, G. D. Jin, D. Chen and X. Y. Hu, *Sens. Actuators, B*, 2009, **138**, 174–181.

26 A. A. Ensafi, M. Taei and T. Khayamian, *Colloids Surf. B*, 2010, **79**, 480–487.

27 B. Y. Zhang, D. K. Huang, X. B Xu, G. Alemu, Y. B. Zhang, F. Zhan, Y. Shen and M. K. Wang, *Electrochem. Acta*, 2013, **91**, 261–266.

28 C. Wang, R. Yuan, Y. Q. Chai, S. H. Chen, Y. Zhang, F. X. Hu and M. H. Zhang, *Electrochem. Acta*, 2012, **62**, 109–115.

29 P. Shakkthivel and S.M. Chen, *Biosens. Bioelectron*., 2007, **22**, 1680–1687.

30 T. Selvaraju and R. Ramaraj, *Electrochem. Acta*, 2007, **52**, 2998–3005.

31 J. F. Ping, J. Wu, Y. X. Wang and Y. B. Ying, *Biosens. Bioelectron*., 2012, **34**, 70–76.

32 M. Amal Raj and S. Abraham John, *J. Phys. Chem. C*, 2013, **117**, 4326–4335.

33 H. L. Qi, X. X. Li, P. Chen and C. X. Zhang, *Talanta*, 2007, **72**, 1030–1035.

34 J. M. Nugent, K. S. V. Santhanam, A. Rubio and P. M. Ajayan, *Nano Lett.*, 2001, **1,** 87–91.

35 A. J. Bard and L. R Faulkner, *Electrochemical Methods—Fundamentals and Application*, John Wiley & Sons, Inc, 2nd edn., 2001, pp. 813.

36 M. G. Zhang and W. Gorski, *J. Am. Chem. Soc.*, 2005, **127**, 2058–2059.

37 H. M. Abu-Shawish, S. M. Saadeh and A. R. Hussien, *Talanta*, 2008, **76**, 941–948.

38 S. Shahrokhian and M. Ghalkhani, *Electrochem. Acta*, 2006, **51**, 2599–2606.

39 Z. F. Chen and Y. B. Zu, J. *Electroanal. Chem*., 2008, **612**, 151–155.

40 L. Zhang, C. H. Zhang and J. Y. Lian, *Biosens. Bioelectron*., 2008, **24**, 690–695.

41 J. M. Zen and P. Chen, *Anal. Chem*., 1997, **69**, 5087–5093.

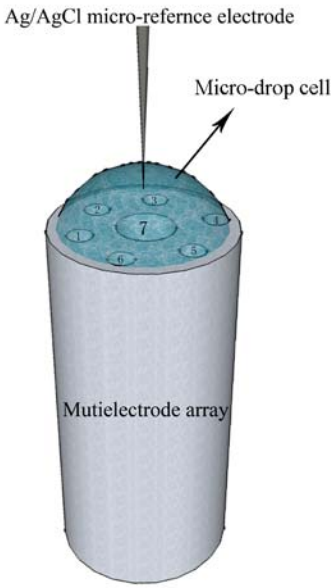

Fig. 1 Schematic diagram of the electrochemical measurement system.

No.1, 2, 3, 4, 5 and 6 holes are the working electrodes; No.7 hole is the counter electrode.

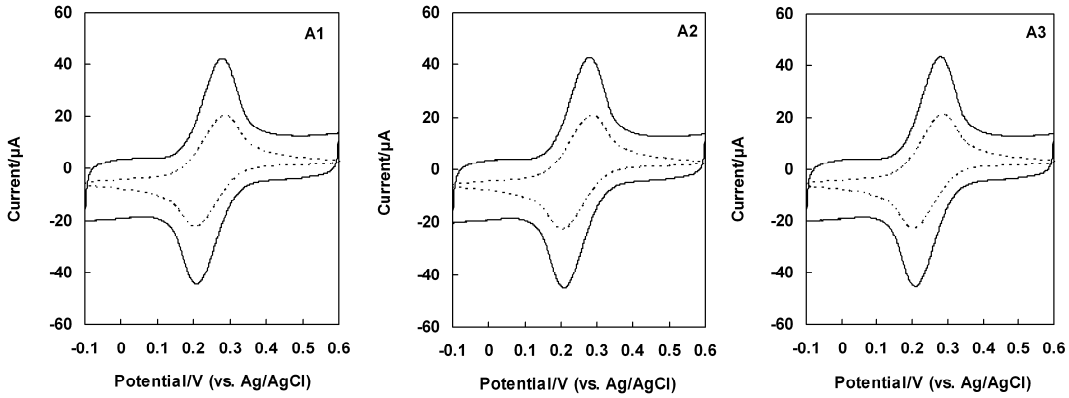

Fig. 2 Cyclic voltammograms of 1.0×10^{-3} M $K_3[Fe(CN)_6]$-0.10 M KCl at the surface of graphite paste multielectrode array (dotted line) and carbon nanotubes paste multielectrode array (solid line). Scan rate, 50 $mV.s^{-1}$

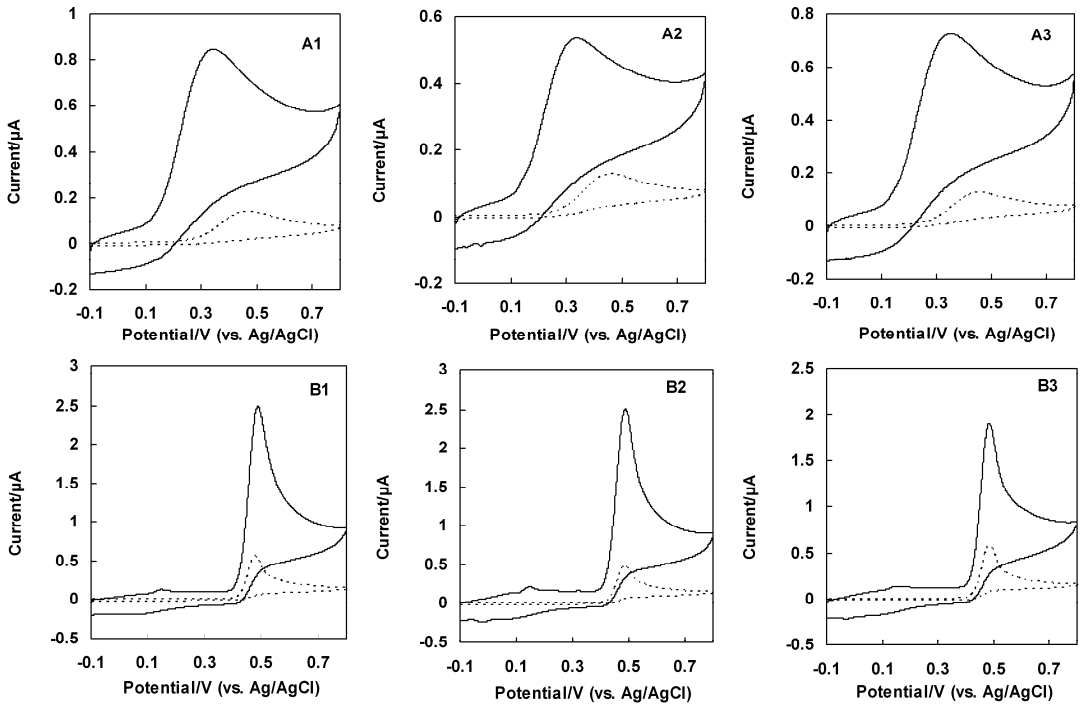

Fig. 3 Cyclic voltammograms of 2.0×10^{-4} M AA (A1, A2, A3) and 2.0×10^{-5} M UA (B1, B2, B3) in 0.10 M acetate buffer solution (pH 5.00) at the surface of carbon nanotubes paste multielectrode array (solid line) and graphite paste multielectrode array (dotted line). Scan rate, 50 $mV.s^{-1}$.

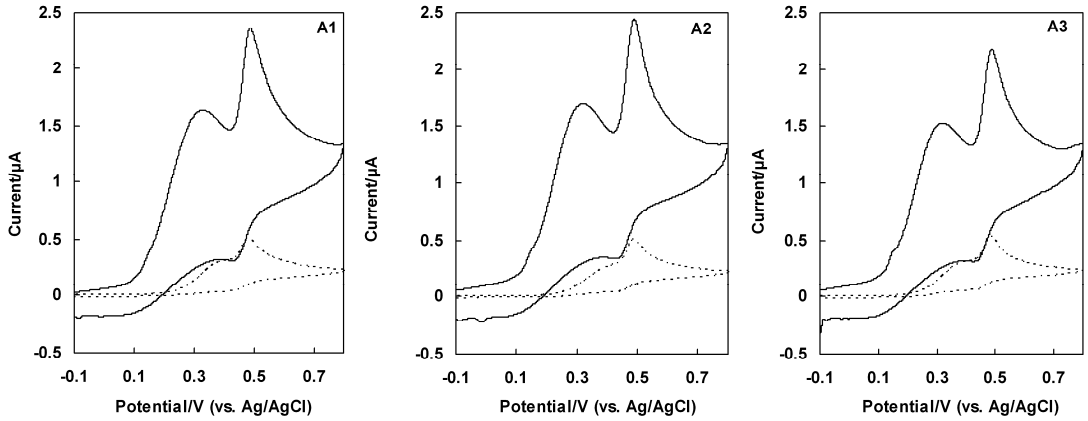

Fig. 4 Cyclic voltammograms (A1, A2, A3) of the mixture containing 2.0×10^{-4} M AA and 2.0×10^{-5} M UA in 0.10 M acetate buffer solution (pH 5.00) at the surface of carbon nanotubes paste multielectrode array (solid line) and graphite paste multielectrode array (dotted line). Scan rate, 50 $mV.s^{-1}$.

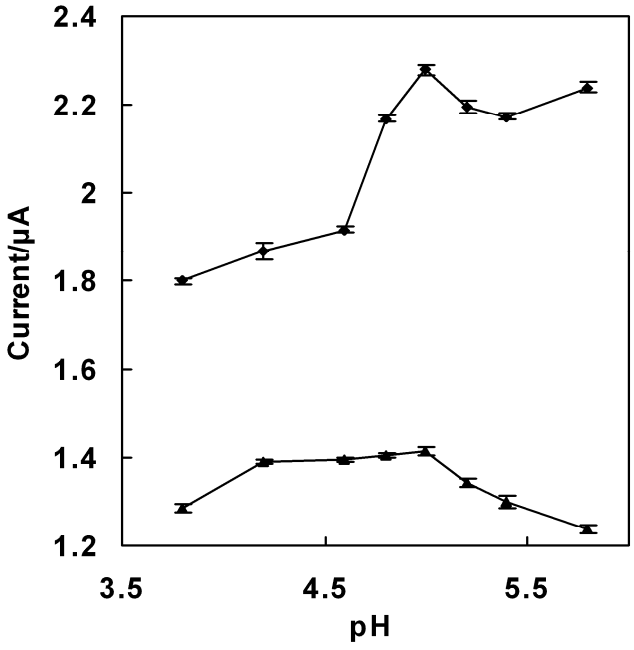

Fig. 5 Effect of pH on the peak current for the oxidation of 6.0×10^{-4} AA and 2.0×10^{-5} UA. Scan rate, 50 $mV.s^{-1}$. The error bars represent the standard deviation of three repeated measurements.

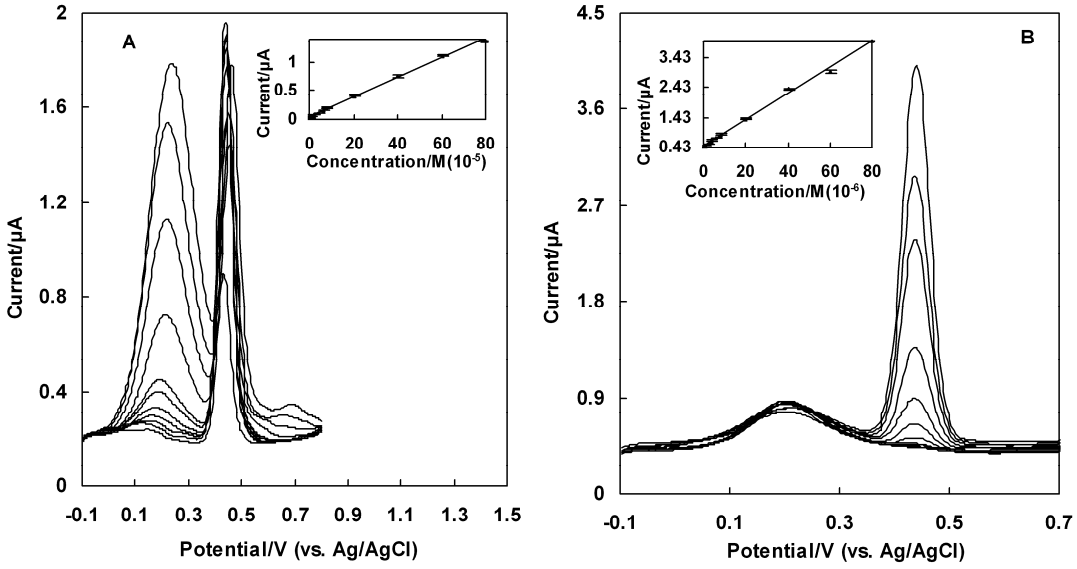

Fig. 6 Square wave voltammograms for the mixture containing AA and UA with different concentrations in 0.10 M acetate buffer (pH 5.00) at the carbon nanotubes paste electrode.

(A) UA (6.0×10^{-6} M) and AA (0, 2.0×10^{-6}, 4.0×10^{-6}, 6.0×10^{-6}, 2.0×10^{-5}, 4.0×10^{-5}, 6.0×10^{-5}, 8.0×10^{-5}, 2.0×10^{-4}, 4.0×10^{-4}, 6.0×10^{-4}, 8.0×10^{-4} M) (down to up); (B) AA (2.0×10^{-4} M) and UA (0, 2.0×10^{-7}, 4.0×10^{-7}, 6.0×10^{-7}, 8.0×10^{-7}, 2.0×10^{-6}, 4.0×10^{-6}, 6.0×10^{-6}, 8.0×10^{-6}, 2.0×10^{-5}, 4.0×10^{-5}, 6.0×10^{-5}, 8.0×10^{-5} M); Supporting electrolyte was 0.10 M acetate (pH 5.00) and pulse amplitude was 25 mV, frequency was 15 Hz. Inset: plots of the peak currents versus concentration of AA or UA. The error bars represent the standard deviation of three repeated measurements.

Table 1 Uric acid determinations in urine samples and human serum at the surface of carbon nanotubes paste multielectrode array

Sample No	Sample preparation	UA found[a] (μM)	Recovery (%)	Reference[38] (μM)
	Human urine	24.58(±0.5)	_	24.90(±0.7)
1	Sample 1+8.0 μM UA	32.98(±0.8)	104	_
2	Sample 1+20 μM UA	44.49(±1.1)	100	_
	Human serum	3.98(±0.3)	_	3.68(±0.11)
3	Sample 2 + 6.0 μM UA	9.91(±0.7)	99	_
4	Sample 2 + 8.0 μM UA	11.44(±0.6)	97	_

[a] Average of five determinations.